Meshless singular boundary method for two-dimensional pseudo-parabolic equation: analysis of stability and convergence

Mohammad Aslefallah[1] · Saeid Abbasbandy[1] · Elyas Shivanian[1]

Abstract

In this study, the singular boundary method is applied to solve time-dependent pseudo-parabolic equations in two space dimensions with initial and Dirichlet-type boundary conditions. A splitting procedure is used to split the solution of the inhomogeneous governing equation into a homogeneous solution and a particular solution. This work presents the numerical operation for calculating the particular solution and homogeneous solution. Several numerical examples are provided to show the accuracy and efficiency of the method. Furthermore, the analysis of stability and convergence is presented.

1 Introduction

We consider third order two-dimensional equation on the domain Ω as follows:

$$\frac{\partial u}{\partial t} - \alpha \Delta u - \eta \frac{\partial}{\partial t}(\Delta u) = f(\mathbf{x}, t), \quad \text{in } \Omega \times (0, T], \tag{1}$$

$$u(\mathbf{x}, 0) = g(\mathbf{x}), \quad \text{in } \Omega, \tag{2}$$

$$u(\mathbf{x}, t) = h(\mathbf{x}, t), \quad \text{on } \partial\Omega, \tag{3}$$

where Δ is the two-dimensional Laplacian, $\Omega \subseteq \mathbb{R}^2$ and $\partial\Omega$ is the boundary of Ω. Also, functions f and g are known continuous functions and α, η and $T > 0$ are specified constants. Moreover, the function $h(\mathbf{x}, t)$ is a known smooth function. When

✉ Mohammad Aslefallah
  maslefallah@gmail.com

1   Department of Applied Mathematics, Faculty of Sciences, Imam Khomeini International University, Qazvin 34149-16818, Iran

$\eta = 0$, as special case of Eq. (1), the equation is the 2D time-dependent diffusion equation.

These equations belong to family of pseudo-parabolic or Sobolev type equations, that emerge in engineering fields like heat conduction including a thermodynamic temperature and a conductive temperature, flows of fluids via fissured rock and quasi-stationary operations in semi-conductors [1–3].

Several finite element and finite volume approaches have been made to handle for 1D and 2D problems [3–7]. Other numerical techniques such as family of finite differences and spectral and methods for this kind of equations can be seen in [8,9]. Comparing with the finite element method (FEM), the finite volume method (FVM) and the boundary element method (BEM), meshfree methods are used to stablish system of algebraic equations for whole problem domain with no need to mesh of the domain discretization in order to use a set of points scattered inside the domain of the problem such as sets of points on the boundaries of the domain to state the domain of the problem and its boundaries. Moreover, some meshless methods are based on of collocation techniques like the meshless collocation method by using radial basis functions (RBFs) [10–13] and some other kinds of meshfree methods is based on weak forms and hybrid of collocation approach and weak forms, like the element free Galerkin (EFG) method [14,15] and the meshless local Petrov–Galerkin (MLPG) method [16–18]. Another approach has been applied for numerical solution of differential equations is spectral collocation method like spectral meshless radial point interpolation (SMRPI) method [19]. Also, there are some novel meshless methods [20–22]. Against to the domain-type meshless methods as methods based on collocation approaches, there are several boundary-type methods like the method of fundamental solutions (MFS), boundary collocation method (BCM), regularized meshless method (RMM) and boundary knot method (BKM) [23–29].

Recently, Chen et al. proposed the singular boundary method (SBM) as a meshfree boundary collocation method [30–36].

The SBM directly uses the fundamental solutions as basis functions and it omits the artificial boundary problem in the MFS. The main concept in the SBM is to present the notion of origin intensity factors (OIFs) to remove the singularities of fundamental solutions on the adaptation of the source points and collocation points upon physical boundary of domain. The SBM is easy in mathematically speaking, simple for programming, accurate and free of integration, more enforceable for problems on complicated shapes with high dimension domains, less time-consuming than the boundary element method (BEM) and at the same time keeps away the fictitious boundary in the MFS and becomes numerically more stable than the MFS because condition number of its interpolation matrix is better [37–40]. As well as the MFS and BEM, the SBM acts when the fundamental solution of the defined problem is attainable [41–46]. The SBM applies the fundamental solution as the basis function. The important concept of the SBM is to utilize the OIF to substitute the singular integration in the BEM to gain accurate numerical consequences, while keeping high numerical stability and also it has less computation load. Specially, the SBM can achieve to high accurate numerical results employing very few boundary points and small CPU time.

There are some ways have been extended to calculate the OIFs. The first approach is named the inverse interpolation technique(IIT), in numerical form, calculates OIFs.

The second technique is to conclude the analytical formula for evaluating unknown OIFs. And the third one is empirical approach to determining OIFs. In this paper, subtracting and adding-back (SAB) technique is a popular approach to calculate the OIFs that it is more fast and stable than the IIT.

The structure of this article is organized as follows: In Sect. 2, we express briefly mathematical preliminaries and numerical implementation of the method. In Sect. 3, we present time discretization and implementation of method on Eqs. (1)–(3). Section 4 includes discussion for analysis of stability and convergence of the method. Also we obtain an error estimate under some conditions. Some numerical examples are reviewed to show the accuracy of the method,and results are reported in Sect. 5. Finally, in the last section, a concluding remarks are given.

2 Mathematical preliminaries and numerical implementations

This section deals with the numerical procedure in order to calculating the particular solution and homogeneous solution. For approximation particular solution and homogeneous solution we applied MPS method and SBM method, respectively.

2.1 Method of particular solutions (MPS)

An important category of problem-dependent radial basis functions are particular solutions [47–49]. By applying splitting scheme, the solution of the inhomogeneous governing equation split into homogeneous solution and particular solution. The key point is to make the particular solutions to satisfy the governing equation.

Consider the boundary value problem as follows:

$$\Re u(\mathbf{x}) = \psi(\mathbf{x}), \quad \mathbf{x} \in \Omega, \tag{4}$$

$$\mathfrak{B}u(\mathbf{x}) = \omega(\mathbf{x}), \quad \mathbf{x} \in \Gamma, \tag{5}$$

where $\Re$ is a differential operator, $\mathfrak{B}$ is a boundary differential operator, ψ and ω are given functions, Ω and $\Gamma = \partial\Omega$ are the inner region and boundary of the domain, respectively.

Suppose $\mathbf{x}_i{}_{i=1}^N$ are the interpolation points containing N_i interior points in Ω and N_b boundary points on Γ, so $N = N_i + N_b$.

If u_p be a particular solution of Eq. (4), then it satisfies

$$\Re u_p(\mathbf{x}) = \psi(\mathbf{x}), \quad \mathbf{x} \in \Omega, \tag{6}$$

but has not necessary need to satisfy the boundary condition. If u_p in Eq. (6) can be achieved, then the main equation in Eqs. (4) and (5) can be turned into the following homogeneous equation via the variable substitution $u_h = u - u_p$, namely

$$\Re u_h(\mathbf{x}) = 0, \quad \mathbf{x} \in \Omega, \tag{7}$$

$$\mathfrak{B}u_h(\mathbf{x}) = \omega(\mathbf{x}) - \mathfrak{B}u_p(\mathbf{x}), \quad \mathbf{x} \in \Gamma. \tag{8}$$

The homogeneous equation Eqs. (7) and (8) can be solved by using boundary methods. The above numerical approach for solving partial differential equations is pretty standard provided when the particular solution and fundamental solution are both attainable. The final solution of Eqs. (4) and (5)can be attained by summation of particular solution and homogeneous solution as follows:

$$u = u_p + u_h.$$

The method of particular solution (MPS) is used for the discretization of the Eqs. (4) and (5). By MPS, for approximating the variable ψ by a linear superposition of the radial basis functions (RBFs), we consider the solution to Eqs. (4) and (5) can be approximated by a linear superposition of the corresponding particular solutions of the given radial basis function like ϕ, such as

$$\psi(\mathbf{x}) = \sum_{j=1}^{N} \alpha_j \phi(||\mathbf{x} - \mathbf{x}_j||), \tag{9}$$

where $||.||$ is the Euclidean norm, α_j are the undetermined coefficients, an approximate particular solution u_p to Eq. (6) as follows

$$u_p(\mathbf{x}) = \sum_{j=1}^{N} \alpha_j \Phi(||\mathbf{x} - \mathbf{x}_j||), \tag{10}$$

where

$$\Re\Phi = \phi. \tag{11}$$

2.2 Particular solution for modified Helmholtz equation

In this work, we utilize Polyharmonic splines of higher order or generalized thin plate spline (GTPS) as radial basis functions, described as:

$$\phi(r) = r^m \ln(r), \qquad m = 2, 4, 6, \ldots \ in \ \mathbb{R}^2. \tag{12}$$

For modified Helmholtz operator as: $\Re = \Delta - \mu^2$ and considering Eqs. (11) and (12) we obtain:

$$(\Delta - \mu^2)\Phi(r) = \phi(r), \tag{13}$$

where Δ states the Laplace operator. Finally [47]–[49], we get

$$\Phi(r) = -\frac{1}{\mu^2} \sum_{i=1}^{m/2} \left(\frac{\Delta}{\mu^2}\right)^i . r^m \ln(r) - \frac{(m)!!^2}{\mu^{m+2}} K_0(\mu r), \tag{14}$$

where r is the Euclidean norm between the point $\mathbf{x}$ and the origin. Function K_0 is the Bessel function of the second kind of order zero.

For TPS $\phi(r) = r^2 \ln(r)$ in $\mathbb{R}^2$, means $m = 2$ in Eq. (14), the corresponding particular solution is:

$$\Phi(r) = \begin{cases} -\dfrac{r^2 \ln(r)}{\mu^2} - \dfrac{4}{\mu^4}\left(1 + \ln(r) + K_0(\mu r)\right), & r \neq 0, \\ \dfrac{4}{\mu^4}\left(-1 + \gamma + \ln\left(\dfrac{\mu}{2}\right)\right), & r = 0. \end{cases} \tag{15}$$

And for polyharmonic splines of order 2, $\phi(r) = r^4 \ln(r)$ in $\mathbb{R}^2$, the corresponding particular solution is:

$$\Phi(r) = \begin{cases} -\dfrac{r^4 \ln(r)}{\mu^2} - \dfrac{8r^2\left(2\ln(r) + 1\right)}{\mu^4} - \dfrac{\left(96 + 64\ln(r) + 64K_0(\mu r)\right)}{\mu^6}, & r \neq 0, \\ \dfrac{1}{\mu^6}\left(-96 + 64\gamma + 64\ln\left(\dfrac{\mu}{2}\right)\right), & r = 0. \end{cases} \tag{16}$$

In (15) and (16) constant γ, is the Euler constant equal to

$$\gamma = 0.57721566490153286\ldots$$

Remark 2.1 For calculating Laplace of u_p by Eqs. (10) and (13), it can result in

$$\Delta u_p(\mathbf{x}) = \sum_{j=1}^{N} \alpha_j \Delta\Phi(r_j), \tag{17}$$

and

$$\Delta\Phi(r_j) = \mu^2 \Phi(r_j) + \phi(r_j), \tag{18}$$

finally, by merging two above equations we get:

$$\Delta u_p(\mathbf{x}) = \sum_{j=1}^{N} \alpha_j \left(\mu^2 \Phi(r_j) + \phi(r_j)\right). \tag{19}$$

2.3 Singular boundary method (SBM)

The SBM belongs to the classification of boundary-type meshless methods based on the singular fundamental solution that uses as the basis function of its approximation expansion. In contrast with the MFS, the source points of the SBM are located upon the physical boundary that are coincided with collocation points while in MFS the source points are located over a fictitious boundary. The main idea in the SBM is to present the notion of origin intensity factors (OIFs) to omit the singularities of fundamental solutions on the adaptation of the source and collocation points on physical boundary of domain.

Consider the homogenous PDE with the following conditions:

$$\begin{cases} \mathfrak{R}u = 0, & \mathbf{x} \in \Omega \subset \mathbb{R}^n, \\ u = g_0(\mathbf{x}), & \mathbf{x} \in \Gamma_D, \\ q(\mathbf{x}) = \dfrac{\partial u(\mathbf{x})}{\partial \mathbf{n}} = g_1(\mathbf{x}), & \mathbf{x} \in \Gamma_N, \end{cases} \tag{20}$$

that $\mathfrak{R}$ is a partial differential operator, $\mathbf{n}$ is the unit outward normal vector, Ω states the computational domain that it is a bounded and connected known domain, Γ_D and Γ_N illustrate the Dirichlet boundary (essential) and the Neumann boundary (natural) conditions, $\Gamma_D \cup \Gamma_N = \partial \Omega$ and $\Gamma_D \cap \Gamma_N = \varnothing$, that $\partial \Omega$ represents the whole physical boundary. Also, functions $g_0(\mathbf{x})$ and $g_1(\mathbf{x})$ are given functions.

The SBM approximates the solution $u(x)$ by a linear combination of the fundamental solution as its basis function. If $G(\mathbf{x})$ be the fundamental solution of the operator in Eq. (20), for field points $\mathbf{x}_i$ and source points $\mathbf{s}_j$, approximation of u and q are:

$$u(\mathbf{x}_i) = \sum_{j=1}^{N} \alpha_j G(\mathbf{x}_i, \mathbf{s}_j), \qquad \mathbf{x} \in \Omega - \Gamma_D, \tag{21}$$

$$u(\mathbf{x}_i) = \sum_{j=1, i \neq j}^{N} \alpha_j G(\mathbf{x}_i, \mathbf{s}_j) + \alpha_i u_{ii}, \qquad \mathbf{x} \in \Gamma_D, \tag{22}$$

$$q(\mathbf{x}_i) = \sum_{j=1, i \neq j}^{N} \alpha_j \frac{\partial G(\mathbf{x}_i, \mathbf{s}_j)}{\partial \mathbf{n}} + \alpha_i q_{ii}, \qquad \mathbf{x} \in \Gamma_N, \tag{23}$$

where N is the number of source points and α_j is the jth unknown coefficient. Singularities of the fundamental solution G will occur when $\mathbf{x}_i = \mathbf{s}_j$. To eliminate this problem, the SBM recommends the notion of origin intensity factors (OIFs). The method places all computing points on the same physical boundary. So the source points $\mathbf{s}_j$ and the collocation points $\mathbf{x}_i$ are the same set of boundary nodes. When $\mathbf{x}_i = \mathbf{s}_j$, we use origin intensity factors replacing the singular terms in formulation. Where u_{ii} and q_{ii} in Eqs. (22) and (23) are defined as the OIFs corresponding to the fundamental solutions and the unit outward normal of fundamental solutions, namely, the diagonal elements of the SBM interpolation matrix. Therefore, to solve all kinds of physical and mechanical problems, the main issue is to specify the OIFs. The origin intensity factor is numerically assigned by the inverse interpolation technique (IIT), where a sample solution u_s satisfying the governing equation are imperative, and some sample points $\mathbf{y}_k$ are located inside of the physical domain.

By using subtracting and adding-back (SAB) technique presented in [33], SBM interpolation formula for boundary condition can be regularized accurately.

The origin intensity factor is numerically determined, where a sample solution u_s satisfying the governing equation are imperative, and some sample points $\mathbf{y}_k$ are located inside the physical domain.

Replacing the sample points $\mathbf{y}_k$ with the boundary collocation points $\mathbf{x}_i$, the SBM interpolation matrix of the diffusion problem can be written as

$$u_s(\mathbf{x}_i) = \sum_{j=1, j\neq i}^{N} \beta_j G(\mathbf{x}_i, \mathbf{s}_j) + \beta_j u_{ii}, \tag{24}$$

and

$$\frac{\partial u_s(\mathbf{x}_i)}{\partial \mathbf{n}} = \sum_{j=1, j\neq i}^{N} \beta_j \frac{\partial G(\mathbf{x}_i, \mathbf{s}_j)}{\partial \mathbf{n}} + \beta_j q_{ii}, \tag{25}$$

It is noted that only the origin intensity factors u_{ii} and q_{ii} are unknown in the above equation. Thus, the origin intensity factors can be calculated via

$$u_{ii} = \frac{1}{\beta_i} \left[u_s(\mathbf{x}_i) - \sum_{j=1, j\neq i}^{N} \beta_j G(\mathbf{x}_i, \mathbf{s}_j) \right], \tag{26}$$

and

$$q_{ii} = -\frac{1}{L_i} \sum_{j=1, j\neq i}^{N} L_j \frac{\partial G_0(\mathbf{x}_i, \mathbf{s}_j)}{\partial n_s}, \tag{27}$$

where L_i is the half length of the curve between source points $\mathbf{s}_{i-1}$ and $\mathbf{s}_{i+1}$. Also G_0 is the fundamental solution of the Laplace equation in 2D.

It is noted that the sample points $\mathbf{y}_k$ do not coincide with the source points $\mathbf{s}_j$, and the sample points number should not be fewer than the physical boundary source node number.

Finally, the approximated solution is:

$$u(\mathbf{x}) = \sum_{j=1, i\neq j}^{N} \alpha_j G(\mathbf{x}, \mathbf{s}_j) + \alpha_i u_{ii}, \tag{28}$$

that, Eq. 28 is the solution of equation Eq. 20.

It is emphasized that the source intensity factors only depends on the distribution of the source points, the fundamental solution of the governing equation and the boundary conditions. Theoretically speaking, the source intensity factors remain unchanged with different sample solutions. Therefore, by employing mentioned technique, we circumvent the singularity of the fundamental solution upon the coincidence of the source and collocation points.

Remark 2.2 (Improved singular boundary method with moment condition) The SBM formulation applies well for some problems. For better result for the problem which solution contains a constant potential, in modified approach, the ISBM method add a constant term to the SBM expansion formula (28) to insure the uniqueness of the SBM interpolation matrix. In [34] the ISBM formulation is defined by

$$u(\mathbf{x}) = \sum_{j=1, i \neq j}^{N} \alpha_j G(\mathbf{x}, \mathbf{s}_j) + \alpha_i u_{ii} + \alpha_{N+1} \tag{29}$$

with the condition

$$\sum_{j=1}^{N} \alpha_j = 0. \tag{30}$$

Remark 2.3 For the Laplace equation on 2D domain, as

$$\Delta u(\mathbf{x}) = 0, \quad \mathbf{x} \in \Omega, \tag{31}$$

fundamental solution described as following formula:

$$G(\mathbf{x}, \mathbf{s}_j) = -\frac{1}{2\pi} \ln(r(\mathbf{x}, \mathbf{s}_j)) = -\frac{1}{2\pi} \ln(\|\mathbf{x} - \mathbf{s}_j\|_2), \quad \mathbf{x} \in \mathbb{R}^2, \tag{32}$$

where r defined above.

Remark 2.4 For the modified Helmholtz equation on a two-dimensional domain, as

$$(\Delta - \mu^2) u(\mathbf{x}) = 0, \quad \mathbf{x} \in \Omega, \tag{33}$$

fundamental solution can be written by the following formula:

$$G(\mathbf{x}, \mathbf{s}_j) = -\frac{1}{2\pi} K_0(\mu r(\mathbf{x}, \mathbf{s}_j)) = -\frac{1}{2\pi} K_0(\mu \|\mathbf{x} - \mathbf{s}_j\|_2), \quad \mathbf{x} \in \mathbb{R}^2, \tag{34}$$

where r and K_0 defined above.

Remark 2.5 Relation between OIFs of Laplace and modified Helmholtz operators: In [30] shown that the origin intensity factors (OIFs) of the modified Helmholtz equation are relevant with the OIFs of the Laplace equation as following relations:

$$u^{ii} = u_L^{ii} - \frac{1}{2\pi} \ln\left(\frac{\mu}{2}\right) - \frac{\gamma}{2\pi}, \tag{35}$$
$$q^{ii} = q_L^{ii}, \tag{36}$$

where u_L^{ii} and q_L^{ii} are OIFs in Dirichlet and Neumann boundary conditions of the Laplace equation respectively. Also, γ is the Euler constant.

Remark 2.6 (Uniqueness of solution of the modified Helmholtz equation) If Ω be a bounded domain and solutions u_1 and u_2 be solutions of the modified Helmholtz equation, then, $w := u_1 - u_2$ satisfies:

$$(\Delta - \mu^2) w(\mathbf{x}) = 0, \quad \mathbf{x} \in \Omega, \tag{37}$$

and

$$w(\mathbf{x}) = 0, \qquad \mathbf{x} \in \partial\Omega,$$ (38)

by multiplying above equation by w, integrating over Ω, and applying Green's first identity we obtain:

$$\int_\Omega w \Delta w \, d\mathbf{x} - \mu^2 \int_\Omega w^2 \, d\mathbf{x} = 0,$$

$$\left(\int_{\partial\Omega} w \frac{\partial w}{\partial n} \, ds - \int_\Omega |\nabla w|^2 \, d\mathbf{x} \right) - \mu^2 \int_\Omega w^2 \, d\mathbf{x} = 0,$$

$$\int_\Omega |\nabla w|^2 \, d\mathbf{x} + \mu^2 \int_\Omega w^2 \, d\mathbf{x} = 0,$$

which acquires that $w = 0$ and therefore $u_1 = u_2$.

3 Finite differences for time discretization

In this section, by introducing a uniformly partitioned time mesh, the procedure of time discretization based on the forward finite-difference relation will be used for approximation of the first order derivative on time variable of the main equation at two successive time levels k and $k + 1$ as follows:

Let $\delta t = t^{k+1} - t^k$ be the constant length of the time steps and $t^k = k\delta t$. For any $t^k \leq t \leq t^{k+1}$:

$$\frac{\partial u^k}{\partial t} \cong \frac{u^{k+1}(\mathbf{x}) - u^k(\mathbf{x})}{\delta t},$$ (39)

and for other term in Eq. (1) derivative on time variable described as

$$\frac{\partial}{\partial t}(\Delta u^k) \cong \frac{\Delta u^{k+1}(\mathbf{x}) - \Delta u^k(\mathbf{x})}{\delta t},$$ (40)

that $u^k = u(\mathbf{x}, k\delta t)$. Also, we employ θ-method $(0 \leq \theta \leq 1)$ for the following approximation as

$$\Delta u(\mathbf{x}, t) \cong \theta \Delta u^{k+1}(\mathbf{x}) + (1 - \theta) \Delta u^k(\mathbf{x}).$$ (41)

In special case, if $\theta = \frac{1}{2}$, the Crank–Nicolson technique is:

$$\Delta u(\mathbf{x}, t) \cong \frac{1}{2} \left(\Delta u^{k+1}(\mathbf{x}) + \Delta u^k(\mathbf{x}) \right),$$ (42)

where $\Delta u^k(\mathbf{x}) = \Delta u(\mathbf{x}, k \, \delta t)$, that:

$$\Delta u = \frac{\partial^2 u}{\partial x^2} + \frac{\partial^2 u}{\partial y^2}.$$ (43)

By replacing Eqs. (39)–(42) in Eq. (1), the main equation can be described as:

$$\frac{u^{k+1} - u^k}{\delta t} - \frac{\alpha}{2}\left(\Delta u^{k+1} + \Delta u^k\right) - \frac{\eta}{\delta t}\left(\Delta u^{k+1} - \Delta u^k\right) = \frac{f^{k+1} + f^k}{2} + R^{k+1},$$

(44)

in which $|R^{k+1}| < C\delta t$, that C is a positive constant.

Then by omitting the small term R^{k+1}, we obtain the following equation:

$$\left(\frac{\alpha}{2} + \frac{\eta}{\delta t}\right)\Delta u^{k+1} - \frac{1}{\delta t}u^{k+1} = \left(\frac{\eta}{\delta t} - \frac{\alpha}{2}\right)\Delta u^k - \frac{1}{\delta t}u^k - \frac{f^{k+1} + f^k}{2}. \quad (45)$$

Suppose that $\lambda = \frac{\alpha}{2} + \frac{\eta}{\delta t}$, $\mu^2 = \frac{1}{\delta t \lambda}$ and $F^{k+1} = -\frac{f^{k+1} + f^k}{2\lambda}$, therefore, we get

$$\Delta u^{k+1} - \mu^2 u^{k+1} = \frac{1}{\lambda}\left(\frac{\eta}{\delta t} - \frac{\alpha}{2}\right)\Delta u^k - \mu^2 u^k + F^{k+1}. \quad (46)$$

If the right hand side of Eq. (46) demonstrated as a function like $b^k(\mathbf{x})$, with condition $\lambda > 0$, Eq. (46) can be rewritten as modified Helmholtz equation as follows:

$$(\Delta - \mu^2)u^{k+1}(\mathbf{x}) = b^k(\mathbf{x}), \quad (47)$$

where

$$b^k(\mathbf{x}) = \frac{1}{\lambda}\left(\frac{\eta}{\delta t} - \frac{\alpha}{2}\right)\Delta u^k - \mu^2 u^k + F^{k+1}. \quad (48)$$

Notice that for $k = 0$, from Eq. (48) and initial condition $u^0 = u(\mathbf{x}, 0) = g_0$ we obtain:

$$b^0(\mathbf{x}) = \frac{1}{\lambda}\left(\frac{\eta}{\delta t} - \frac{\alpha}{2}\right)\Delta g_0 - \mu^2 g_0 + F^1, \quad (49)$$

4 Analysis of stability and convergence

For analysis of the stability and convergence of Eq. (46) with considered initial condition $u(\mathbf{x}, 0) = u^0$, and boundary condition $u^k|_{\partial\Omega} = u(\mathbf{x}, t_k), k = 0, 1, \ldots, n$, consider the inner product as follows:

$$(u, v) = \int_\Omega u(\mathbf{x})v(\mathbf{x})d\mathbf{x}, \quad (50)$$

and norm in L^2

$$\|u\|_2 = [(u, u)]^{1/2} = \left[\int_\Omega u^2(\mathbf{x})d\mathbf{x}\right]^{1/2}. \quad (51)$$

For the finite-difference scheme (46), some results achieved as follows:

Theorem 4.1 *Suppose $u^k \in H_0^2(\Omega), k = 0, 1, \ldots, n$ is the solution of Eq. (46), if the functions $\frac{\partial u^k}{\partial x}$ and $\frac{\partial u^k}{\partial y}$ are monotone function with respect to variable t, and $\alpha\delta t > 2\eta$*

then

$$\|u^k\|_2 \leq \|u^0\|_2 + max_{0 \leq j \leq n} \|F^j\|_2.$$

Proof The theorem proven by mathematical induction. For $k = 0$, it is clear that

$$\Delta u^1 - \mu^2 u^1 = \frac{1}{\lambda}\left(\frac{\eta}{\delta t} - \frac{\alpha}{2}\right)\Delta u^0 - \mu^2 u^0 + F^1. \tag{52}$$

If Eq. (52) multiply by u^1 and integrating on Ω then

$$(\Delta u^1, u^1) - \mu^2(u^1, u^1) = \frac{1}{\lambda}\left(\frac{\eta}{\delta t} - \frac{\alpha}{2}\right)(\Delta u^0, u^1) - \mu^2(u^0, u^1) + (F^1, u^1). \tag{53}$$

By employing of Green's formula as follows:

$$\int_\Omega \nabla u \cdot \nabla v \mathrm{d}\mathbf{x} = \int_{\partial\Omega} u \frac{\partial v}{\partial \mathbf{n}} \mathrm{d}s - \int_\Omega u \Delta v \mathrm{d}\mathbf{x},$$

where

$$\frac{\partial v}{\partial \mathbf{n}} = \frac{\partial v}{\partial x} n_1 + \frac{\partial v}{\partial y} n_2$$

is the outward normal derivative on the boundary $\partial\Omega$, we obtain

$$(\nabla u^1, \nabla u^1) + \mu^2(u^1, u^1) = \frac{1}{\lambda}\left(\frac{\eta}{\delta t} - \frac{\alpha}{2}\right)(\nabla u^0, \nabla u^1) + \mu^2(u^0, u^1) - (F^1, u^1), \tag{54}$$

and then,

$$\|u^1\|_2^2 + \frac{1}{\mu^2}(\nabla u^1, \nabla u^1) = (u^0, u^1) + \frac{1}{\lambda\mu^2}\left(\frac{\eta}{\delta t} - \frac{\alpha}{2}\right)(\nabla u^0, \nabla u^1) - \frac{1}{\mu^2}(F^1, u^1), \tag{55}$$

where, it has been used from this fact that $u^1 \in H_0^2(\Omega)$. Since $\alpha\delta t > 2\eta$ and the functions $\frac{\partial u^k}{\partial x}$ and $\frac{\partial u^k}{\partial y}$ are monotone functions with respect to variable t, then $2\eta - \alpha\delta t < 0$ and $(\nabla u^1, \nabla u^0) > 0$. Hence, Eq. (55) yields

$$\|u^1\|_2^2 \leq (u^0, u^1) + (F^1, u^1). \tag{56}$$

Finally, by applying Schwarz inequality, we have

$$\|u^1\|_2 \leq \|u^0\|_2 + \|F^1\|_2 \leq \|u^0\|_2 + max_{0 \leq j \leq n}\|F^j\|_2. \tag{57}$$

For hypothesis of mathematical induction suppose we have proven following inequality:

$$\|u^l\|_2 \leq \|u^0\|_2 + max_{0 \leq j \leq n}\|F^j\|_2, \quad l = 1, 2, \ldots, k. \tag{58}$$

If Eq. (46) multiply by u^{k+1} and integrating on Ω then

$$(\Delta u^{k+1}, u^{k+1}) - \mu^2(u^{k+1}, u^{k+1}) = \frac{1}{\lambda}\left(\frac{\eta}{\delta t} - \frac{\alpha}{2}\right)(\Delta u^k, u^{k+1})$$
$$- \mu^2(u^k, u^{k+1}) + (F^{k+1}, u^{k+1}), \tag{59}$$

using Green's formula leads to

$$(\nabla u^{k+1}, \nabla u^{k+1}) + \mu^2(u^{k+1}, u^{k+1}) = \frac{1}{\lambda}\left(\frac{\eta}{\delta t} - \frac{\alpha}{2}\right)(\nabla u^k, \nabla u^{k+1})$$
$$+ \mu^2(u^k, u^{k+1}) - (F^{k+1}, u^{k+1}), \tag{60}$$

and then,

$$\|u^{k+1}\|_2^2 + \frac{1}{\mu^2}(\nabla u^{k+1}, \nabla u^{k+1}) = (u^k, u^{k+1})$$
$$+ \frac{1}{\lambda\mu^2}\left(\frac{\eta}{\delta t} - \frac{\alpha}{2}\right)(\nabla u^k, \nabla u^{k+1}) - \frac{1}{\mu^2}(F^{k+1}, u^{k+1}). \tag{61}$$

Now by applying theorems's assumptions and Schwarz inequality, it results in

$$\|u^{k+1}\|_2 \leq \|u^k\|_2 + \|F^{k+1}\|_2, \tag{62}$$

and by using (58), we obtain

$$\|u^{k+1}\|_2 \leq \|u^0\|_2 + max_{0 \leq j \leq n}\|F^j\|_2, \tag{63}$$

hence, the proof is complete. $\qquad\square$

Suppose that U^k is the solution of Eq. (46) with the initial condition $u(\mathbf{x}, 0) = U^0$, and the boundary condition $U^k|_{\partial\Omega} = u(\mathbf{x}, t_k)$, then the stability resultant can be expressed as follows.

Theorem 4.2 *The time discrete numerical solution Eq. (46) is H^1-convergent with convergence order $O(\delta t)$*

Proof Define the error

$$\epsilon(\mathbf{x}) = u^k(\mathbf{x}) - U^k(\mathbf{x}),$$

it satisfies

$$\Delta\epsilon^{k+1}(\mathbf{x}) - \mu^2\epsilon^{k+1}(\mathbf{x}) = \frac{1}{\lambda}\left(\frac{\eta}{\delta t} - \frac{\alpha}{2}\right)\Delta\epsilon^k(\mathbf{x}) - \mu^2\epsilon^k(\mathbf{x})$$

and

$$\epsilon^{k+1}|_{\partial\Omega} = 0.$$

By usage of Theorem 4.1, we have

$$\|\epsilon^k\|_2 \leq \|\epsilon^0\|_2, \qquad k = 1, 2, \ldots, n,$$

hence, the proof is complete. □

Now we perform an error estimate for the approximated solution of the time-discretized equation (46). We signify from now by C a general constant that can not be the same at different occasions.

Theorem 4.3 *Under assumptions of Theorem 4.1, suppose $\{u_e(\mathbf{x}, t^k)\}_{k=0}^{k=n}$ be the exact solution of the problem* (1)–(3), *and $\{u(\mathbf{x}, t^k)\}_{k=0}^{k=n}$ be the approximated solution Eq.* (46) *with considered initial condition $u_e(\mathbf{x}, 0) = u(\mathbf{x}, 0)$, then error estimates can be stated as follows*

$$\|u_e(\mathbf{x}, k\delta t) - u(\mathbf{x}, k\delta t)\|_2 \leq C(\delta t). \tag{64}$$

Proof As regards $u_e(\mathbf{x}, t^k)$ is the exact solution of the main equation (1)–(3) and by using Crank–Nicolson method to achieve Eq. (46), then

$$\Delta u_e^{k+1}(\mathbf{x}) - \mu^2 u_e^{k+1}(\mathbf{x}) = \frac{1}{\lambda}\left(\frac{\eta}{\delta t} - \frac{\alpha}{2}\right)\Delta u_e^k(\mathbf{x}) - \mu^2 u_e^k(\mathbf{x}) - F^{k+1} + C(\delta t). \tag{65}$$

Let $\varepsilon^k(\mathbf{x}) = u_e(\mathbf{x}, t^k) - u(\mathbf{x}, t^k)$, by subtracting Eqs. (46) and (65), we acquire

$$\Delta \varepsilon^{k+1}(\mathbf{x}) - \mu^2 \varepsilon^{k+1}(\mathbf{x}) = \frac{1}{\lambda}\left(\frac{\eta}{\delta t} - \frac{\alpha}{2}\right)\Delta \varepsilon^k(\mathbf{x}) - \mu^2 \varepsilon^k(\mathbf{x}) - F^{k+1} + C(\delta t), \tag{66}$$

$$\varepsilon^0(\mathbf{x}) = 0, \quad \varepsilon^0(\mathbf{x})\Big|_{\partial\Omega} = 0. \tag{67}$$

Therefore, from Theorem 4.1, we deduce

$$\|\varepsilon^k(\mathbf{x})\|_2 \leq \|\varepsilon^0(\mathbf{x})\|_2 + C(\delta t) = C(\delta t), \tag{68}$$

then

$$\|u_e(\mathbf{x}, t^k) - u(\mathbf{x}, t^k)\|_2 \leq C(\delta t), \tag{69}$$

hence, the proof is complete. □

5 Numerical experiments

In this section we present the numerical examples acquired by employing the Singular boundary method for approximated solution of the 2D pseudoparabolic problems.

We solve four examples using the SBM method mentioned in Sect. 2, and report the numerical results.

The accuracy and convergency of the method shown with two types of error measurements, maximum absolute error ε_∞ and relative error ε_R are used as follows:

$$\varepsilon_\infty(u) = \|u_{exact} - u_{approx}\|_\infty, \tag{70}$$

or

$$\varepsilon_\infty(u) = \max\{|u_{exact}(\mathbf{x}_i, t) - u_{approx}(\mathbf{x}_i, t)|, i = 1, 2, \ldots, N\},$$

and

$$\varepsilon_R(u) = \sqrt{\frac{\sum_{i=1}^{N}(u_{exact}(\mathbf{x}_i, t) - u_{approx}(\mathbf{x}_i, t))^2}{\sum_{i=1}^{N}(u_{exact}(\mathbf{x}_i, t))^2}}, \tag{71}$$

where $u_{exact}(\mathbf{x}_i, t)$ and $u_{approx}(\mathbf{x}_i, t)$ denote exact and numerical approximated solutions, respectively.

In the following examples we employ Polyharmonic splines of order 2 described as: $\phi(r) = r^4 ln(r)$, as radial basis function.

Example 1 On a finite square $\Omega_1 = [0, 1]^2$, consider Eqs. (1)–(3) with initial condition

$$u(\mathbf{x}, 0) = \cos x + \sin y, \quad \mathbf{x} \in [0, 1] \times [0, 1] \tag{72}$$

and boundary conditions

$$\begin{array}{ll} u(x, 0, t) = e^{2t}\cos x, & u(x, 1, t) = e^{2t}(\cos x + \sin(1)), \\ u(0, y, t) = e^{2t}(1 + \sin y), & u(1, y, t) = e^{2t}(\cos(1) + \sin y), \end{array} \tag{73}$$

where the analytical solution is: $u(\mathbf{x}, t) = e^{2t}(\cos x + \sin y)$, and $f(\mathbf{x}, t) = (2 + \alpha + 2\eta)e^{2t}(\cos x + \sin y)$.

Here, the presented approach is applied for numerical solution of the main problem with $\alpha = 1$ and $\eta = 0.00025$. Two kinds of errors are reported in Table 1 at different times until the desired time $t = 1$. Furthermore, it is clear from Table 1 that $\varepsilon_R(u)$ of SBM method has no growth whenever the time is increasing, in the other words, this fact shows that the method is stable. The numerical approximated solution obtained by the SBM and the maximum absolute error of this computed solution with $\delta t = 0.001$ and $N = 441$ at time $T = 1$ are shown in Fig. 1 which discloses the validity and accuracy of this method. Figure 2 shows the comparison between SBM and SMRPI methods for behaviour of $\varepsilon_\infty(u)$ (left) and behaviour of $\varepsilon_R(u)$ (right) with $\delta t = 0.001$ and $N = 441$ at time $t \in [0, 1]$.

Example 2 In the next case, consider Eqs. (1)–(3) on the circular physical domain Ω_2, which is described by

$$\Omega_2 = \left\{ \mathbf{x} = (x, y) \in \mathbb{R}^2 : \sqrt{x^2 + y^2} \leq 3 \right\}$$

with initial condition $u(\mathbf{x}, 0) = \cos x + \sin y, \quad \mathbf{x} \in \Omega_2$, and boundary conditions, where the analytical solution is: $u(\mathbf{x}, t) = e^{2t}(\cos x + \sin y)$, and $f(\mathbf{x}, t) = (2 + \alpha + 2\eta)e^{2t}(\cos x + \sin y)$.

Table 1 The $\varepsilon_\infty(u)$ and $\varepsilon_R(u)$ errors obtained by SBM and compared by SMRPI with N=441 and $\delta t = 0.001$ at time t for Example 1

| t	$\varepsilon_\infty(u)$		$\varepsilon_R(u)$	
	SBM	SMRPI [19]	SBM	SMRPI [19]
0.10	1.1566×10^{-3}	3.0755×10^{-3}	5.4282×10^{-4}	6.2135×10^{-4}
0.20	1.1650×10^{-3}	3.7662×10^{-3}	5.4214×10^{-4}	6.2740×10^{-4}
0.30	1.0926×10^{-3}	4.6011×10^{-3}	5.4139×10^{-4}	6.2794×10^{-4}
0.40	1.0161×10^{-3}	4.9199×10^{-3}	5.4053×10^{-4}	6.2800×10^{-4}
0.50	1.0082×10^{-3}	5.3642×10^{-3}	5.3953×10^{-4}	6.2800×10^{-4}
0.60	1.0018×10^{-3}	5.9839×10^{-3}	5.3836×10^{-4}	6.2800×10^{-4}
0.70	1.5911×10^{-3}	6.0240×10^{-3}	5.3697×10^{-4}	6.2800×10^{-4}
0.80	2.6354×10^{-3}	7.2507×10^{-3}	5.3534×10^{-4}	6.2800×10^{-4}
0.90	3.9023×10^{-3}	8.1276×10^{-3}	5.3346×10^{-4}	6.2800×10^{-4}
1.00	5.4020×10^{-3}	8.8658×10^{-3}	5.3130×10^{-4}	6.2800×10^{-4}
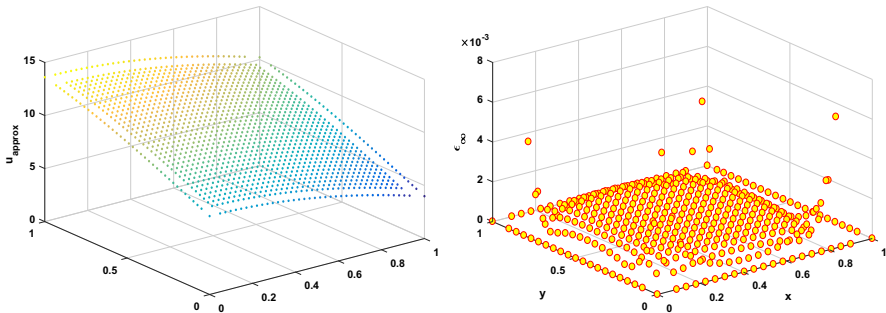
Fig. 1 Approximate solution by SBM (left) and behaviour of $\varepsilon_\infty(u)$ (right) with $\delta t = 0.001$ and $N = 441$ at time $T = 1$ for Example 1
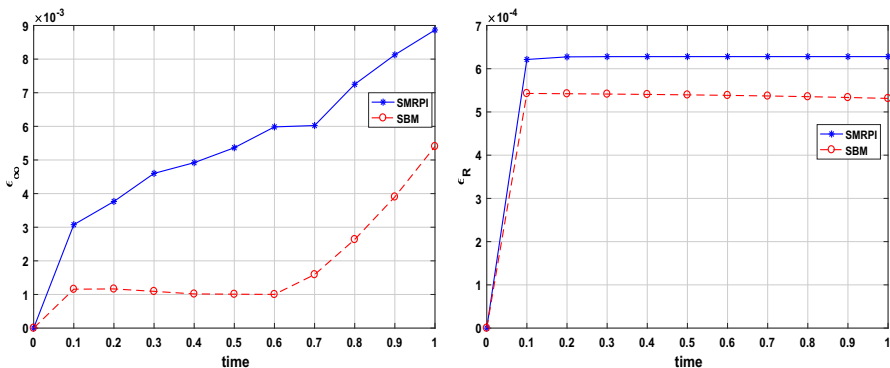

Fig. 2 Comparison SBM and SMRPI for behaviour of $\varepsilon_\infty(u)$ (left) and behaviour of $\varepsilon_R(u)$ (right) at different time $t \in [0, 1]$ for with $\delta t = 0.001$ and $N = 441$ for Example 1

Table 2 The $\varepsilon_\infty(u)$ and $\varepsilon_R(u)$ errors obtained by SBM with N=441 and different δt at time t for example 2

| t	$\delta t = 0.01$		$\delta t = 0.005$	
	$\varepsilon_\infty(u)$	$\varepsilon_R(u)$	$\varepsilon_\infty(u)$	$\varepsilon_R(u)$
0.10	1.4890×10^{-3}	7.4502×10^{-4}	9.4808×10^{-5}	1.7249×10^{-5}
0.20	1.4845×10^{-3}	7.3847×10^{-4}	1.4723×10^{-4}	2.7356×10^{-5}
0.30	1.4803×10^{-3}	7.2991×10^{-4}	1.5930×10^{-4}	3.0956×10^{-5}
0.40	1.4761×10^{-3}	7.2102×10^{-4}	1.4302×10^{-4}	2.8605×10^{-5}
0.50	1.4719×10^{-3}	7.1521×10^{-4}	9.7010×10^{-5}	2.1041×10^{-5}
0.60	1.4616×10^{-3}	7.1727×10^{-4}	5.9018×10^{-5}	1.1487×10^{-5}
0.70	1.9180×10^{-3}	7.3284×10^{-4}	1.0733×10^{-4}	1.8600×10^{-5}
0.80	2.5066×10^{-3}	7.6742×10^{-4}	2.3303×10^{-4}	4.1052×10^{-5}
0.90	3.1820×10^{-3}	8.2527×10^{-4}	3.8462×10^{-4}	6.9831×10^{-5}
1.00	3.9428×10^{-3}	9.0854×10^{-4}	5.6146×10^{-4}	1.0373×10^{-4}
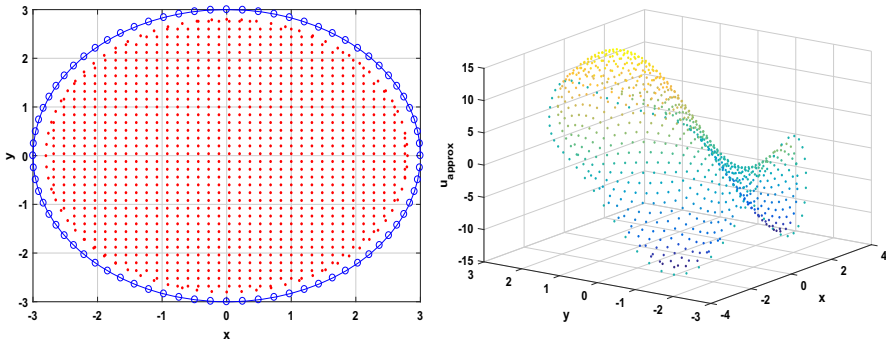
Fig. 3 Domain of the problem (left) and numerical solution by SBM (right) with $\delta t = 0.005$ and $N = 441$ for example 2

Here, the presented approach is applied for numerical solution of the problem with $\alpha = 1$ and $\eta = 0.00025$. Two kinds of errors are reported in Table 2 at different times until the favorable time $T = 1$. As it is shown, the numerical results are valid. Furthermore, it is obvious from Table 2 that $\varepsilon_R(u)$ has no growth whenever the time is increasing, namely this shows that the method is stable. The uniform point distribution of the domain Ω and numerical solution achieved by the SBM with $\delta t = 0.005$ and $N = 441$ at time T=1 are shown in Fig. 3. Also, Fig. 4 shows the behaviour of $\varepsilon_\infty(u)$ with $\delta t = 0.01$ and $N = 441$ at time T=1.

Example 3 In this example, the computational domain is the amoeba-like physical domain, Ω_3, which is described by

$$\Omega_3 = \left\{ (r\cos\theta, r\sin\theta) : r = e^{\sin\theta}\sin^2(2\theta) + e^{\cos\theta}\cos^2(2\theta) \right\}$$
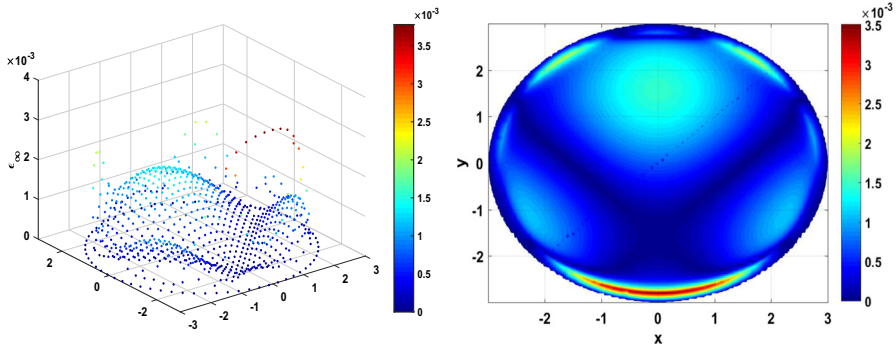
Fig. 4 Graphs of maximum absolute error as surface plot (left) and contour plot (right) for behaviour of $\varepsilon_\infty(u)$ with $\delta t = 0.01$ and $N = 441$ at time $T = 1$ for Example 2

Here, we consider Eqs. (1)–(3) upon Ω_3 with initial condition

$$u(\mathbf{x}, 0) = \cos x + \sin y, \qquad \mathbf{x} \in \Omega_3,$$

and boundary conditions, where the analytical solution is: $u(\mathbf{x}, t) = e^{2t}(\cos x + \sin y)$, and $f(\mathbf{x}, t) = (2 + \alpha + 2\eta)e^{2t}(\cos x + \sin y)$.

Here, the presented approach is applied for numerical solution of the problem with $\alpha = 1$ and $\eta = 0.00025$. Two kinds of the errors are reported in Table 3 at different times until the desired time $t = 1$. Furthermore, it is obvious from Table 3 that $\varepsilon_R(u)$ has no growth whenever the time is increasing, that means the method is stable. Also, these errors show that the presented methodology is efficient and accurate for the evaluation of the problem. The uniform point distribution of the domain Ω and numerical solution obtained by the SBM with $\delta t = 0.005$ and $N = 441$ at time $T=1$ are shown in Fig. 5. Moreover, Fig. 6 shows the behaviour of $\varepsilon_\infty(u)$ with $\delta t = 0.01$ and $N = 441$ at time $T=1$.

Example 4 As another example, the SBM is employed to solve the problem. To illustrate the accuracy of this method, a more complex multiply connected domain is considered and the collocation points are distributed regularly, in the irregular physical domain Ω_4, which is described by

$$\Omega_4 = \left\{ (r\cos\theta, r\sin\theta) : r = m^2 + 5m + 2 - \frac{2m+2}{m^3}\cos(m\theta) \right\}$$

for $m = 6$. According to Eqs. (1)–(3) on Ω_4 with initial condition

$$u(\mathbf{x}, 0) = \cos x + \sin y, \qquad (x, y) \in \Omega_4, \tag{74}$$

and boundary conditions, the analytical solution is: $u(\mathbf{x}, t) = e^{2t}(\cos x + \sin y)$, and $f(\mathbf{x}, t) = (2 + \alpha + 2\eta)e^{2t}(\cos x + \sin y)$.

Table 3 The $\varepsilon_\infty(u)$ and $\varepsilon_R(u)$ errors obtained by SBM with N=441 and different δt at time t for example 3

| t	$\delta t = 0.01$		$\delta t = 0.005$	
	$\varepsilon_\infty(u)$	$\varepsilon_R(u)$	$\varepsilon_\infty(u)$	$\varepsilon_R(u)$
0.10	1.4446×10^{-3}	7.4871×10^{-4}	2.0419×10^{-4}	6.9974×10^{-6}
0.20	1.6613×10^{-3}	7.4749×10^{-4}	2.6603×10^{-4}	1.2422×10^{-5}
0.30	2.4795×10^{-3}	7.4659×10^{-4}	4.0940×10^{-4}	1.6603×10^{-5}
0.40	3.4438×10^{-3}	7.4632×10^{-4}	7.2555×10^{-4}	1.9946×10^{-5}
0.50	4.5464×10^{-3}	7.4679×10^{-4}	1.1196×10^{-3}	2.2965×10^{-5}
0.60	6.9230×10^{-3}	7.4883×10^{-4}	1.7610×10^{-3}	2.6281×10^{-5}
0.70	9.7664×10^{-3}	7.5302×10^{-4}	2.5333×10^{-3}	3.0539×10^{-5}
0.80	1.2989×10^{-2}	7.6018×10^{-4}	3.4217×10^{-3}	3.6265×10^{-5}
0.90	1.6581×10^{-2}	7.7711×10^{-4}	4.4216×10^{-3}	4.3786×10^{-5}
1.00	2.0532×10^{-2}	7.8696×10^{-4}	5.5292×10^{-3}	5.3232×10^{-5}
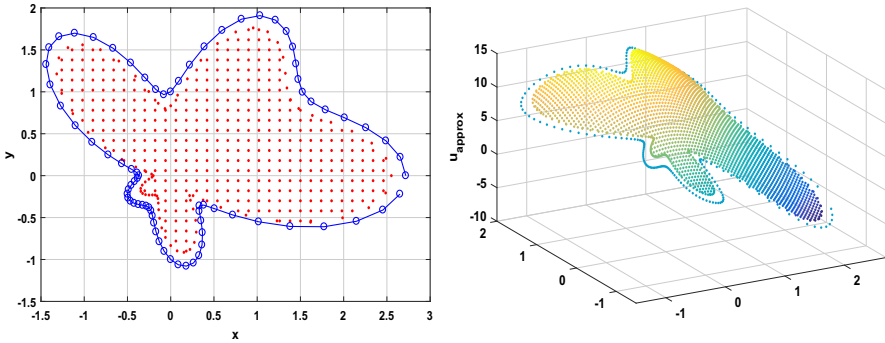
Fig. 5 Domain of the problem (left) and numerical solution by SBM (right) with $\delta t = 0.005$ and $N = 441$ for Example 3
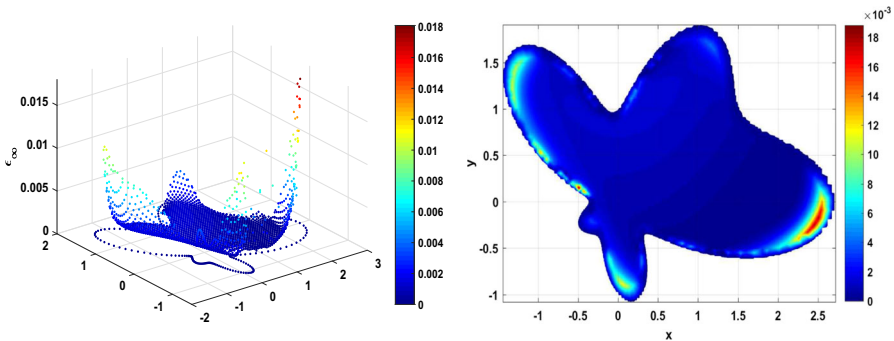

Fig. 6 Graphs of maximum absolute error as surface plot (left) and contour plot (right) for behaviour of $\varepsilon_\infty(u)$ with $\delta t = 0.01$ and $N = 441$ at time $T = 1$ for Example 3

Table 4 The $\varepsilon_\infty(u)$ and $\varepsilon_R(u)$ errors calculated by SBM with N=441 and different δt at time t for Example 4

| t | $\delta t = 0.01$ | | $\delta t = 0.005$ | |
	$\varepsilon_\infty(u)$	$\varepsilon_R(u)$	$\varepsilon_\infty(u)$	$\varepsilon_R(u)$
0.10	3.1625×10^{-4}	7.5448×10^{-5}	4.1081×10^{-5}	1.6569×10^{-6}
0.20	9.1407×10^{-4}	7.8911×10^{-5}	1.2720×10^{-4}	2.9022×10^{-6}
0.30	1.8465×10^{-3}	8.7706×10^{-5}	3.4071×10^{-4}	4.6787×10^{-6}
0.40	3.2214×10^{-3}	1.0387×10^{-4}	6.4957×10^{-4}	8.0416×10^{-6}
0.50	4.9675×10^{-3}	1.2865×10^{-4}	1.0509×10^{-3}	1.3356×10^{-5}
0.60	7.0901×10^{-3}	1.6244×10^{-4}	1.5432×10^{-3}	2.0662×10^{-5}
0.70	9.5977×10^{-3}	2.0523×10^{-4}	2.1258×10^{-3}	2.9957×10^{-5}
0.80	1.2500×10^{-2}	2.5694×10^{-4}	2.7984×10^{-3}	4.1259×10^{-5}
0.90	1.5811×10^{-2}	3.1755×10^{-4}	3.5615×10^{-3}	5.4580×10^{-5}
1.00	1.1954×10^{-2}	3.8710×10^{-4}	4.4155×10^{-3}	6.9948×10^{-5}
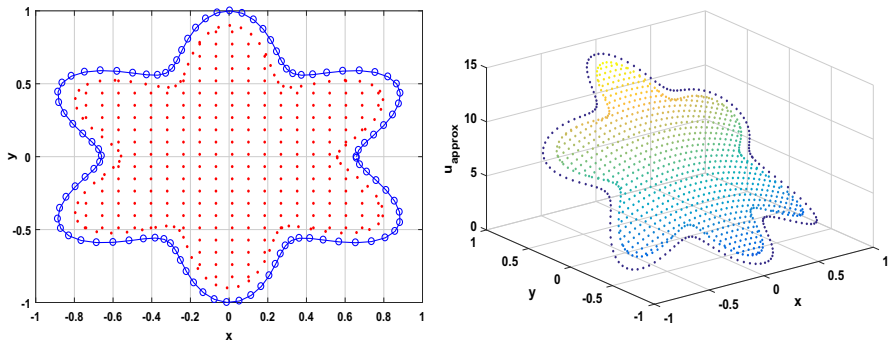
Fig. 7 Domain of the problem (left) and numerical solution by SBM (right) for Example 4 with $\delta t = 0.005$ and $N = 441$

Here, the presented approach is applied for numerical solution of the problem with $\alpha = 1$ and $\eta = 0.00025$. Two types of the errors are reported in Table 4 at different times until the desired time $t = 1$. Furthermore, it is clear from Table 4 that $\varepsilon_R(u)$ has no growth whenever the time is increasing, this fact shows the stability of the method.

The uniform point distribution of the domain Ω and numerical solution obtained by the SBM with $\delta t = 0.005$ and $N = 441$ at time T=1 are shown in Fig. 7. Also, Fig. 8 shows the behaviour of $\varepsilon_\infty(u)$ with $\delta t = 0.01$ and $N = 441$ at time $T = 1$.
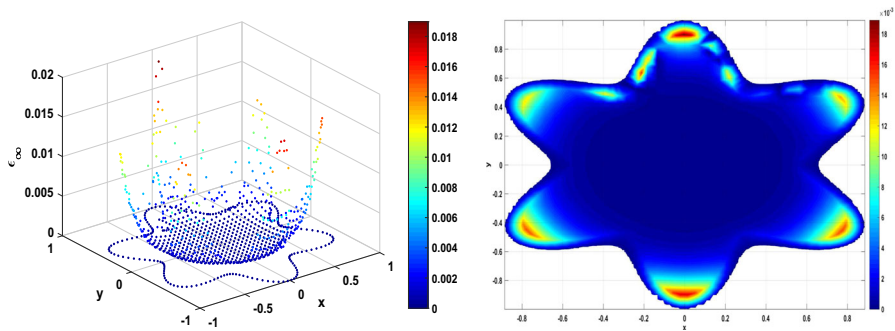
Fig. 8 Graphs of maximum absolute error as surface plot (left) and contour plot (right) for behaviour of $\varepsilon_\infty(u)$ for Example 4 with $\delta t = 0.01$ and $N = 441$ at time $T = 1$

6 Conclusion

In this paper singular boundary method (SBM) has been employed to solve two-dimensional pseudo-parabolic equations. A time discretization was applied to approximate the time derivatives. Also, to illustrate the accuracy and efficiency of this method, four numerical examples with different domains have been presented. Through numerical experiments, we find that SBM results are in good agreement with the exact analytical solutions. The analysis of stability and convergence for this meshless technique have been considered and it has been proved theoretically that technique is stable with respect to some conditions and furthermore, it is convergence. As illustrated by the computational results, the implementation of the proposed method is very easy for similar problems.

References

1. Amiraliyev, G., Mamedov, Y.D.: Difference schemes on the uniform mesh for singular perturbed pseudo-parabolic equations. Turk. J. Math. **19**, 207–222 (1995)
2. Barenblatt, G.I., Entov, V.M., Ryzhik, V.M.: Theory of Fluid Flows Through Natural Rocks. Kluwer Academic Publishers, Dordrecht (1990)
3. Ewing, R.E.: Numerical solution of Sobolev partial differential equations. SIAM J. Numer. Anal. **12**, 345–363 (1975)
4. Arnold, D.N., Douglas, J., Thomee, V.: Superconvergence of a finite element approximation to the solution of a sobolev equation in a single space variable. Math. Comput. **36**, 53–63 (1981)
5. Liu, T., Lin, Y., Rao, M., Cannon, J.: Finite element methods for Sobolev equations. J. Comput. Math. **20**, 627–642 (2002)
6. Yang, M.: Analysis of second order finite volume element methods for pseudo-parabolic equations in three spatial dimensions. Appl. Math. Comput. **196**, 94–104 (2008)
7. Lin, Q., Zhang, S.: A direct global superconvergence analysis for Sobolev and viscoelasticity type equations. Appl. Math. **42**, 23–34 (1997)
8. Quarteroni, A.: Fourier spectral methods for pseudoparabolic equations. SIAM J. Numer. Anal. **24**, 323–335 (1987)
9. Sun, T., Yang, D.: The finite difference streamline diffusion methods for Sobolev equations with convection-dominated term. Appl. Math. Comput. **125**, 325–345 (2002)
10. Han, H., Chen, Q., Qiao, J.: Research on an online self-organizing radial basis function neural network. Neural Comput. Appl. **19**, 667–676 (2010)

11. Dey, P., Gopal, M., Pradhan, P., Pal, T.: On robustness of radial basis function network with input perturbation. Neural Comput. Appl. **31**, 523–537 (2019)
12. Aslefallah, M., Shivanian, E.: Nonlinear fractional integro-differential reaction-diffusion equation via radial basis functions. Eur. Phys. J. Plus **130**, 1–9 (2015)
13. Shivanian, E.: A meshless method based on radial basis and spline interpolation for 2-D and 3-D inhomogeneous biharmonic BVPs. Z. Naturforschung A **70**, 673–682 (2015)
14. Belytschko, T., Lu, Y.Y., Gu, L.: Element free Galerkin methods for static and dynamic fracture. Int. J. Solids Struct. **32**, 2547–2570 (1995)
15. Dehghan, M., Ghesmati, A.: Combination of meshless local weak and strong (MLWS) forms to solve the two dimensional hyperbolic telegraph equation. Eng. Anal. Bound. Elem. **34**, 324–336 (2010)
16. Atluri, S., Zhu, T.: A new meshless local Petrov–Galerkin (MLPG) approach in computational mechanics. Comput. Mech. **22**, 117–127 (1998)
17. Abbasbandy, S., Shirzadi, A.: A meshless method for two-dimensional diffusion equation with an integral condition. Eng. Anal. Bound. Elem. **34**, 1031–1037 (2010)
18. Shivanian, E.: Meshless local Petrov–Galerkin (MLPG) method for three-dimensional nonlinear wave equations via moving least squares approximation. Eng. Anal. Bound. Elem. **50**, 249–257 (2015)
19. Shivanian, E., Aslefallah, M.: Stability and convergence of spectral radial point interpolation method locally applied on two-dimensional pseudoparabolic equation. Numer. Methods Partial Differ. Equ. **33**, 724–741 (2017)
20. Lin, J., Reutskiy, S., Lu, J.: A novel meshless method for fully nonlinear advection-diffusion-reaction problems to model transfer in anisotropic media. Appl. Math. Comput. **339**, 459–476 (2018)
21. Lin, J., Xu, Y., Zhang, Y.: Simulation of linear and nonlinear advection-diffusion-reaction problems by a novel localized scheme. Appl. Math. Lett. **99**, 106005 (2020)
22. Lin, J., Reutskiy, S.: A cubic B-spline semi-analytical method for 3D steady-state convection-diffusion-reaction problems. Appl. Math. Comput. **371**, 124944 (2020)
23. Fairweather, G., Karageorghis, A.: The method of fundamental solutions for elliptic boundary value problems. Adv. Comput. Math. **9**, 69–95 (1998)
24. Golberg, M.A., Chen, C.S., Bowman, H.: Some recent results and proposals for the use of radial basis functions in the BEM. Eng. Anal. Bound. Elem. **23**, 285–296 (1999)
25. Banerjee, P.K.: The Boundary Element Methods in Engineering. McGRAW-HILL Book Company, Berkshire (1994)
26. Marin, L.: Regularized method of fundamental solutions for boundary identification in two-dimensional isotropic linear elasticity. Int. J. Solids Struct. **47**, 3326–3340 (2010)
27. Li, Z.-C., Lee, M.-G., Chiang, J.Y., Liu, Y.P.: The Trefftz method using fundamental solutions for biharmonic equations. J. Comput. Appl. Math. **235**, 4350–4367 (2011)
28. Marin, L., Lesnic, D.: The method of fundamental solutions for the Cauchy problem associated with two-dimensional Helmholtz-type equations. Comput. Struct. **83**, 267–278 (2005)
29. Poullikkas, A., Karageorghis, A., Georgiou, G.: The method of fundamental solutions for three-dimensional elastostatics problems. Comput. Struct. **80**, 365–370 (2002)
30. Chen, W.: Singular boundary method: a novel, simple, mesh-free, boundary collocation numerical method. Chin. J. Solid Mech. **30**, 592–599 (2009)
31. Li, J.P., Chen, W., Fu, Z.J., Sun, L.L.: Explicit empirical formula evaluating original intensity factors of singular boundary method for potential and Helmholtz problems. Eng. Anal. Bound. Elem. **73**, 161–169 (2016)
32. Li, J.P., Chen, W., Fu, Z.J.: Numerical investigation on convergence rate of singular boundary method. Math. Probl. Eng. **2016**, 1–13 (2016)
33. Lin, J., Chen, W., Chen, C.S.: Numerical treatment of acoustic problems with boundary singularities by the singular boundary method. J. Sound Vib. **333**, 3177–3188 (2014)
34. Chen, W., Fu, Z., Wei, X.: Potential problems by singular boundary method satisfying moment condition. CMES **51**, 65–85 (2009)
35. Qu, W.Z., Chen, W., Gu, Y.: Fast multipole accelerated singular boundary method for the 3D Helmholtz equation in low frequency regime. Comput. Math. Appl. **70**, 679–690 (2015)
36. Wang, F., Chen, W., Zhang, C., Lin, J.: Analytical evaluation of the origin intensity factor of time-dependent diffusion fundamental solution for a matrix-free singular boundary method formulation. Appl. Math. Model. **49**, 647–662 (2017)
37. Chen, W., Tanaka, M.: A meshless, integration-free, and boundary-only RBF technique. Comput. Math. Appl. **43**, 379–391 (2002)

38. Young, D.L., Chen, K.H., Lee, C.W.: Novel meshless method for solving the potential problems with arbitrary domain. J. Comput. Phys. **209**, 290–321 (2005)
39. Sarler, B.: Solution of potential flow problems by the modified method of fundamental solutions: formulations with the single layer and the double layer fundamental solutions. Eng. Anal. Bound. Elem. **33**, 1374–1382 (2009)
40. Liu, Y.J.: A new boundary meshfree method with distributed sources. Eng. Anal. Bound. Elem. **34**, 914–919 (2010)
41. Aslefallah, M., Abbasbandy, S., Shivanian, E.: Fractional cable problem in the frame of meshless singular boundary method. Eng. Anal. Bound. Elem. **108**, 124–132 (2019)
42. Gu, Y., Chen, W., Zhang, C.Z.: Singular boundary method for solving plane strain elastostatic problems. Int. J. Solids Struct. **48**, 2549–2556 (2011)
43. Aslefallah, M., Rostamy, D.: Application of the singular boundary method to the two-dimensional telegraph equation on arbitrary domains. J. Eng. Math. **118**(1), 1–14 (2019)
44. Lin, J., Zhang, C., Sun, L., Lu, J.: Simulation of seismic wave scattering by embedded cavities in an elastic half-plane using the novel singular boundary method. Adv. Appl. Math. Mech. **10**, 322–342 (2018)
45. Aslefallah, M., Abbasbandy, S., Shivanian, E.: Meshless formulation to two-dimensional nonlinear problem of generalized Benjamin–Bona–Mahony–Burgers through singular boundary method: Analysis of stability and convergence. Numer. Methods Partial Differ. Equ. **36**(2), 249–267 (2020)
46. Aslefallah, M., Abbasbandy, S., Shivanian, E.: Numerical solution of a modified anomalous diffusion equation with nonlinear source term through meshless singular boundary method. Eng. Anal. Bound. Elem. **107**, 198–207 (2019)
47. Ramachandran, P.A., Balakrishnan, K.: Radial basis functions as approximate particular solutions: review of recent progress. Eng. Anal. Bound. Elem. **24**, 575–582 (2000)
48. Muleshkov, A.S., Golberg, M.A., Chen, C.S.: Particular solutions of Helmholtz-type operators using higher order polyharmonic splines. Comput. Mech. **24**, 411–419 (1999)
49. Chen, C.S., Fan, C.M., Wen, P.H.: The method of approximate particular solutions for solving elliptic problems with variable coefficients. Int. J. Comput. Methods **8**, 545–559 (2011)

Publisher's Note Springer Nature remains neutral with regard to jurisdictional claims in published maps and institutional affiliations.